


Review

Phase Equilibrium Studies of the CaO-MgO-Al₂O₃-SiO₂ System for Iron Blast Furnace Slag: A Review

Jinfa Liao ¹, Gele Qing ² and Baojun Zhao ^{1,3,*}¹ International Institute for Innovation, Jiangxi University of Science and Technology, Nanchang 330013, China; liaojinfa678@outlook.com² Shougang Research Institute of Technology, Beijing 100043, China³ Sustainable Minerals Institute, University of Queensland, Brisbane 4072, Australia

* Correspondence: bzhaob@jxust.edu.cn

Abstract: More and larger blast furnaces have been constructed for ironmaking across the world in recent years due to the advantages of high productivity, high energy efficiency and low cost. Slag plays important role in a blast furnace to produce high-quality hot metal and maintain smooth operations. Liquidus temperatures are the essential information of the slag to avoid the formation of the solid phase during the ironmaking process and slag tapping. The principal components of the iron blast furnace slags can be described by the system CaO-MgO-Al₂O₃-SiO₂. With the significant changes in the raw materials and different requirements of the blast furnace operations, phase equilibria in this slag system have been extensively investigated from different directions. Phase diagrams were presented in various pseudo-ternary and pseudo-binary forms to meet the requirements of wide applications. Reliable thermodynamic modelling is the target of the researchers which can predict accurate liquidus temperatures of the slag. Development of the reliable thermodynamic modelling relies on systematic and accurate experimental data including liquidus temperatures and compositions of the solid solutions. Experimental data on the phase equilibria of the system CaO-MgO-Al₂O₃-SiO₂ are summarised and compared with the thermodynamic predictions which can provide systematic information for the researchers and blast furnace operators.

Keywords: phase equilibrium; CaO-MgO-Al₂O₃-SiO₂; liquidus temperature; ironmaking slag; FactSage



Citation: Liao, J.; Qing, G.; Zhao, B. Phase Equilibrium Studies of the CaO-MgO-Al₂O₃-SiO₂ System for Iron Blast Furnace Slag: A Review. *Metals* **2023**, *13*, 801. <https://doi.org/10.3390/met13040801>

Academic Editor: Fernando Castro

Received: 31 March 2023

Revised: 14 April 2023

Accepted: 17 April 2023

Published: 19 April 2023



Copyright: © 2023 by the authors. Licensee MDPI, Basel, Switzerland. This article is an open access article distributed under the terms and conditions of the Creative Commons Attribution (CC BY) license (<https://creativecommons.org/licenses/by/4.0/>).

1. Introduction

The blast furnace (BF) with hundreds of years of history is still the major technology for ironmaking. Feeds to a BF include metallic ore, coke and flux. The recent developments in BF including the injection of coal and the growing size make the BF operation more complex and challenging. The products from a BF include hot metal (Fe-C alloy), slag and off gas. The slag plays important roles in a BF: (1) collection of the impurities from the feeds; (2) complete separation of hot metal from the slag; (3) efficient removal of sulphur from the hot metal and alkali from the BF and (4) smooth tapping of the hot metal and slag from the BF. The chemical compositions of a BF slag can be represented by the system CaO-MgO-Al₂O₃-SiO₂ where SiO₂ and Al₂O₃ are mainly from iron-bearing materials, coke and coal. CaO and MgO are the flux used to adjust the slag composition [1,2].

Being fully liquid is an essential requirement for both hot metal and slag because the solid phase can significantly increase the bulk viscosity of hot metal or slag. The hot metal bearing carbon has a liquidus temperature below 1200 °C which is much lower than the liquidus temperature of the slag. Therefore, control of the slag temperature inside the BF and on tapping above the liquidus temperature to avoid the formation of a solid phase is always the focus of the fundamental studies for BF slags. Phase diagrams in the system CaO-MgO-Al₂O₃-SiO₂ can be used to predict the liquidus temperature of the BF slags [3,4]. However, it is impossible to describe the liquidus temperatures of the slag in a single-phase diagram for this four-component system. Different forms of the pseudo-ternary and

pseudo-binary phase diagrams have been produced and used to meet the requirements of different BF operations, e.g., utilization of low-grade iron ore and poor-quality coke to reduce the cost, minimized slag mass and low operating temperature to reduce energy consumption and greenhouse gas emission, high basicity slag to remove sulphur and low basicity slag to remove alkali.

The phase equilibrium in the system $\text{CaO-MgO-Al}_2\text{O}_3\text{-SiO}_2$ has been studied extensively by many researchers [5–23] and the phase diagrams were presented in different forms. Muan et al. [24] and the Slag Atlas [25] collected and summarised most of the existing data. Significant discrepancies were reported from these studies that affect the direct use of the phase diagrams. High-temperature experiments to construct multicomponent phase diagrams are time- and cost-consuming. Development of reliable thermodynamic modelling to predict liquidus temperatures is always the target of researchers and metallurgists. In recent years, thermodynamic software such as FactSage 8.2 [26], MTDATA [27] and Thermo-Calc [28] have been developed to predict the liquidus temperatures of the slags. Accurate and systematic experimental data are required to develop and optimize the thermodynamic databases and evaluate the reliability of the predictions.

In this paper, the experimental techniques used in phase equilibrium studies related to the BF slags and the produced phase diagrams are critically reviewed. Applications of different forms of the pseudo-ternary and pseudo-binary phase diagrams are demonstrated to support the metallurgists to properly use these phase diagrams on the BF operations. The predictions of the FactSage 8.2 are compared with the experimental results to evaluate the accuracy of the current thermodynamic software.

2. Research Techniques Used in Phase Equilibria Studies of BF Slag

The components of the BF slag $\text{CaO-MgO-Al}_2\text{O}_3\text{-SiO}_2$ do not have valence changes in the condensed system. High-temperature experiments for the determination of the phase equilibria in this system can be carried out in air. Accurate temperature and phase compositions are the essential data to characterize the phase equilibria of the slag. Different techniques have been used to obtain the liquidus temperatures and compositions of the solid solutions. Various thermodynamic models have also been developed to predict the phase equilibria of the slags.

2.1. Liquidus Temperature

As a silicate-based slag system, the quenching technique was usually used in phase equilibria studies of the BF slags. This technique involves high-temperature equilibration followed by rapid cooling. On quenching, the liquid phase is converted to glass and the solid phases are retained in their shapes and properties. The microstructure of the quenched sample can be observed and the phase compositions can be measured at room temperature.

In earlier studies [5,7], the conventional quenching technique was used to construct the pseudo-ternary phase diagrams. From pure chemicals of CaCO_3 , MgO , Al_2O_3 and SiO_2 , 10 g homogeneous mixtures with accurate compositions were prepared by repeatedly fusing in a Pt crucible, quenching and crushing. The obtained glass was completely crystallized at a temperature of the order of 1000 °C for sufficient time. Approximately 20 mg of the powdered crystalline material was enclosed in a Pt envelope, held at a desired temperature for a sufficient time to attain equilibrium, and quenched in mercury. The phases present in the quenched sample were identified by means of a petrographic microscope and X-ray diffraction techniques. The liquidus temperature was determined between the temperature at which the mixture is all liquid and some lower temperature at which crystals are present in the liquid. Therefore, the liquidus temperature can be approached as closely as desired within the limits of error of the temperature measuring and controlling equipment. Usually, each liquidus temperature determined by this technique is followed by a plus or minus value, indicating the closeness of bracketing of the liquidus temperature by runs. In the studies by Prince [6,8], a similar quenching technique was used. CaCO_3 , MgCO_3 , $\text{Al}_2\text{O}_3 \cdot x\text{H}_2\text{O}$ and silicic acid were used as the starting materials. The carbonates were

oven dried and kept in a desiccator. The $\text{Al}_2\text{O}_3 \cdot x\text{H}_2\text{O}$ was calcined to 1250°C for several hours and used immediately after calcination. The silicic acid was leached with 1:1 HCl in an extractor to remove traces of impurities. After three or four fusions, about 20 mg of powdered glass enclosed in a Pt foil envelope was suspended in a vertical tube furnace for equilibration. A maximum of 90 min at temperatures slightly above 1400°C , to 10 min at temperatures near 1600°C were used for the samples to attain equilibrium. Most of the quenching experiments were carried out for 30 to 60 min. The sample was dropped into water or mercury to achieve rapid quenching. A petrographic microscope was used to identify the phases present in the quenched sample by Prince [8] and the refractive index for each primary phase was given in the results tables. The liquidus composition determined in this technique is the same as that prepared at the beginning of the experiment by assuming the composition does not change during the fusion and equilibration. The accuracy of the liquidus temperature relies on the number of equilibration experiments at different temperatures. A single liquidus point requires several days of careful experiments and the resulting liquidus temperature is usually not located directly on an isotherm.

Gutt et al. [10] and Cavalier et al. [11] used a hot-stage microscope to investigate phase equilibria of BF slags. Several milligrams of the fused slag was used as starting material. The liquidus temperature was determined by direct observation of the primary phase precipitation on cooling or dissolution of the solid phase on heating. Where possible, both the primary phase and the secondary phase crystallizing could be identified by their characteristic crystal growth in the melt. The viscosity of the slag and its slow crystallization/dissolution is one of the limitations of the method.

An improved quenching technique was developed with the application of electron probe microanalysis (EPMA) [17–23,29]. In this technique, pure oxides or carbonates were weighed and mixed according to the experimental plan and pelletized. Then, a 0.1–0.5 g pellet was placed in a Pt or graphite crucible and equilibrated for enough time to achieve equilibrium. The experiments were usually carried out in a vertical tube furnace to enable the samples to drop directly into water after the equilibration. A schematic of the vertical tube furnace is shown in Figure 1. The sample is placed in the hot zone of the furnace next to a thermocouple so that the equilibration temperature can be accurately monitored [13].

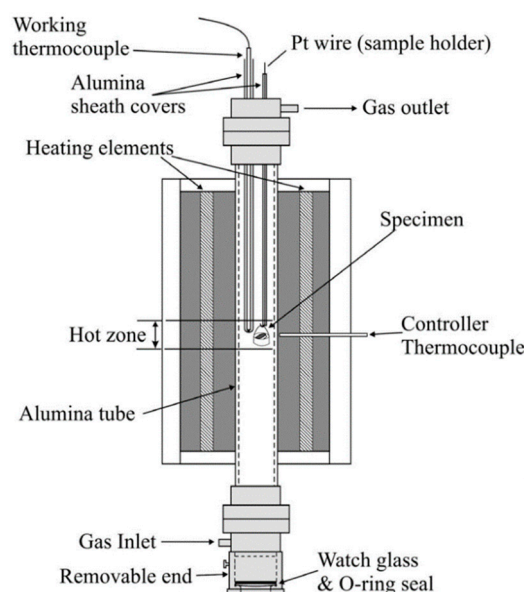


Figure 1. Schematic of tube furnace with specimen for quenching experiments [13].

The equilibrated sample was dropped into water directly to attain rapid cooling. The quenched samples were mounted, polished and carbon-coated for electron probe microanalysis (EPMA). An EPMA with Wavelength Dispersive Spectroscopy (WDS) was

used for microstructural and compositional analyses. The EPMA was operated at an accelerating voltage of 15 kV and a probe current of 15–50 nA. The probe diameter of 1 μm was set to accurately measure the composition of an area larger than 1 μm . The ZAF (Z is atomic number correction factor, A is absorption correction factor, and F is fluorescence correction factor) correction procedure was applied for the data analysis. The standards used for EPMA included alumina (Al_2O_3) for Al, magnesia (MgO) for Mg, and wollastonite (CaSiO_3) for Ca and Si. The average accuracy of the EPMA measurements was within ± 1 wt%. On rapid cooling, the liquid phase in the equilibrated sample was converted to glass and the solid phases were retained in their shapes and compositions. The homogeneity of the phases can be confirmed by the EPMA measurements in different areas of the quenched sample. Usually, 8–20 points of the liquid phase and 3–5 points of the solid phase were measured from different areas by EPMA. The average was taken as the phase composition and the standard deviation was less than 1%. If only the liquid phase is present in the quenched sample, the equilibration temperature needs to be decreased to obtain the which contains both liquid and solid phases. Figure 2 shows examples of the typical microstructures from the quenched samples [22].

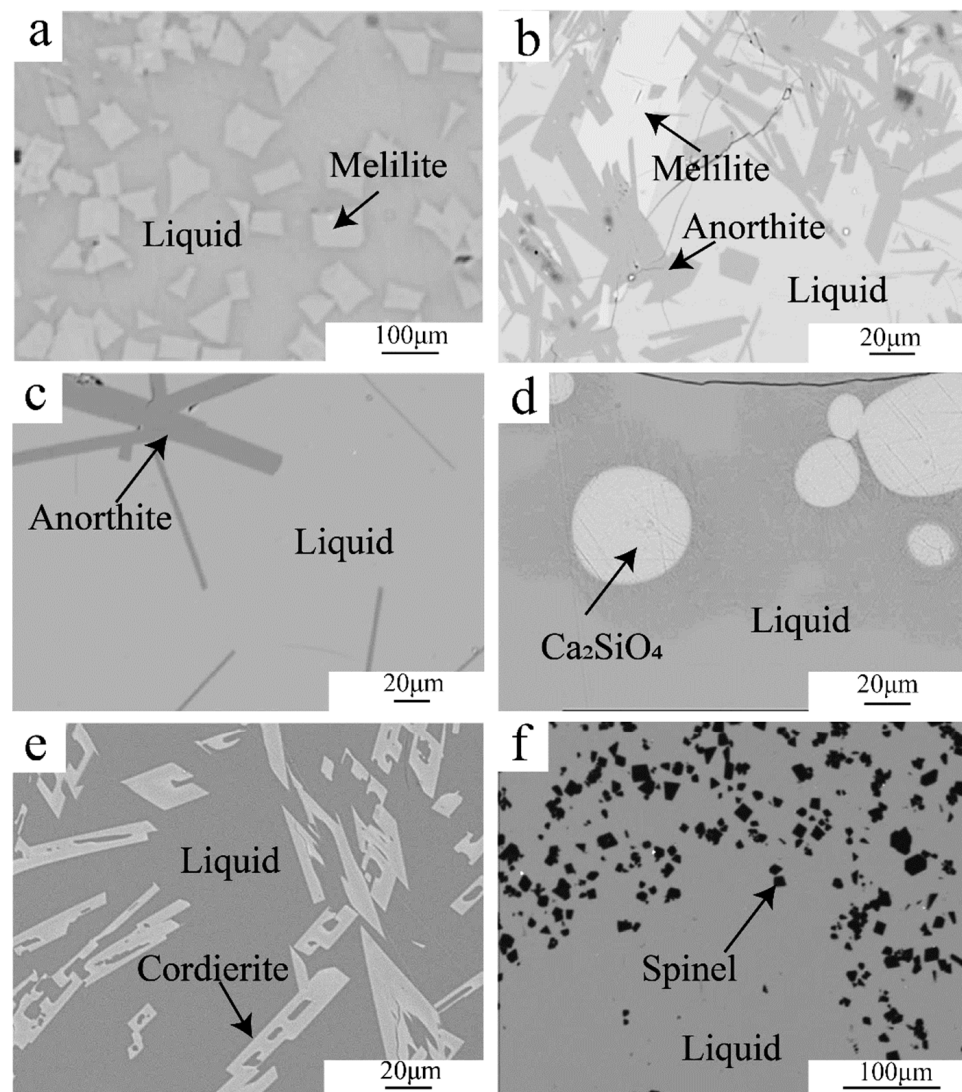


Figure 2. Typical microstructures of the quenched samples showing the equilibrium of liquid with solid phases [22]. (a) melilite, (b) melilite and anorthite, (c) anorthite, (d) Ca_2SiO_4 , (e) cordierite and (f) spinel.

The improved technique has several advantages over the conventional quenching technique. The mixture prepared from pure chemicals can be used directly for equilibration without pre-fusion and crystallization. The equilibration temperature can be fixed to obtain the required isotherms. The compositions of the liquid and solid phases can be measured directly after high-temperature equilibration. Bulk composition change of the sample during the preparation and equilibration does not affect the compositions of the liquid and solid that are used for the construction of the phase diagram. The same mixture can be used to obtain several liquidus points by equilibration at different temperatures. These advantages substantially increased the efficiency and accuracy of phase equilibria determination.

2.2. Solid Solutions

Solid solution data are important for the crystallization and development of thermodynamic modelling. Osborn and Schairer [5] investigated the solid solution between akermanite and gehlenite by petrographic microscope. They observed that the melilite solid solution with 55% akermanite is isotropic in sodium light. Crystals close to this point on the gehlenite side show abnormal blue interference colours in white light. As the proportion of gehlenite is increased, the interference colour continuously changes from bluish-grey to silver-grey to white. By using this technique, the composition of a melilite solid solution with 40–70% akermanite can be estimated from its interference colour with an error of less than $\pm 5\%$ akermanite. Bowen et al. [30] described the detailed procedure to measure the solid solution by petrographic microscope for the system $\text{Ca}_2\text{SiO}_4\text{--Fe}_2\text{SiO}_4$. They also used the X-ray powder diffraction (XRD) method to measure the solubilities of Ca_2SiO_4 in Fe_2SiO_4 . Starting from pure Fe_2SiO_4 , equal steps of the Ca_2SiO_4 content were added and heated at a temperature for enough time. The solubility of Ca_2SiO_4 in Fe_2SiO_4 at a given temperature was determined where the maximum displacement of Fe_2SiO_4 by Ca_2SiO_4 did not change the general characteristics of the diffraction pattern. However, XRD has a limited capacity to detect a trace amount of the second phase which affects the accuracy of the solubility determined by the XRD method.

As seen in Figure 2, rapidly quenched samples contain well-crystallized solid phases together with glass (liquid at the equilibrium temperature). EPMA can accurately measure the compositions of any phases greater than $2\text{ }\mu\text{m}$. In the improved quenching technique, the compositions of liquid with the corresponding solids from the sample are measured simultaneously by EPMA. Accurate liquidus and solidus lines are determined more efficiently than those methods mentioned above where the solubilities were measured in separate experiments.

2.3. Thermodynamic Software

High-temperature experiments are time-consuming and expensive as the construction of a multi-component phase diagram requires a large number of experiments. Thermodynamic modelling has been actively developed and used in recent years to predict the phase equilibria information and understand the chemical reactions more broadly and deeply. As summarized by Jung et al. [31]. A thermodynamic package is developed based on Gibbs energy minimization with continuously improved computational techniques and optimized databases. All available thermodynamic and phase equilibrium data for a given system are critically evaluated simultaneously to obtain one self-consistent set of model equations which can best reproduce the data for all phases as functions of temperature and composition. The accuracy and capacity of a thermodynamic model rely on the number and reliable experimental data available. Where data are lacking for a multicomponent system, the optimized model parameters for low-order (binary and ternary) subsystems can be used to provide initial estimation and the parameters can be evaluated and further optimized when the experimental data of multicomponent systems are available.

The well-known thermochemical software packages used for slag systems include FactSage [26], MTDATA [27] and Thermo-Calc [28]. The user-friendly software enables researchers to perform versatile thermodynamic calculations for wide ranges of slag com-

positions and temperatures. The latest version of FactSage is 8.2 which is one of the most powerful thermodynamic packages for the thermodynamic calculations of the BF slags [32,33]. The databases of “FactPS” and “FToxid” are usually used in the “Equilib” module. The solution phases selected in the calculations of BF slag phase equilibria include “FToxide-SLAGA”, “FToxide-SPINC”, “FToxide-MeO_A”, “FToxide-bC2S”, “FToxide-aC2S”, “FToxide-Mel_A”, “FToxide-WOLLA”, and “FToxide-Mull”.

3. Experimentally Determined Phase Diagrams

A phase diagram for the four-component system $\text{CaO-MgO-Al}_2\text{O}_3\text{-SiO}_2$ needs to be presented in a triangular form of a pseudo-ternary section on a plane. Four major sets of pseudo-ternary phase diagrams have been reported for BF slags. The first set was reported by Osborn et al. [6] and the phase diagrams were presented in the form of pseudo-ternary sections CaO-MgO-SiO_2 at constant Al_2O_3 concentrations. The second set of phase diagrams for BF slags was reported to be the $\text{Al}_2\text{O}_3\text{-CaO-SiO}_2$ pseudo-ternary sections at constant MgO concentrations [8,10,11]. In these early studies, the effects of CaO/SiO_2 ratio and MgO (or Al_2O_3) concentration on liquidus temperatures of the BF slags were discussed and the optimum slag compositions were proposed. In the modern iron BF operation, CaO/SiO_2 ratio is usually fixed for a specific blast furnace. The third set of pseudo-ternary phase diagrams $(\text{CaO} + \text{SiO}_2)\text{-Al}_2\text{O}_3\text{-MgO}$ with constant CaO/SiO_2 ratios of 0.9, 1.1, 1.3 and 1.5 were experimentally determined [13–16]. However, to face the increasing challenge of complex ironmaking raw feeds, the published phase diagrams could not provide enough information. New phase diagrams have been requested from the industry. The pseudo-ternary phase diagrams $(\text{CaO} + \text{MgO})\text{-Al}_2\text{O}_3\text{-SiO}_2$ with constant MgO/CaO ratio of 0.2 and $\text{CaO-MgO-(Al}_2\text{O}_3 + \text{SiO}_2)$ with constant $\text{Al}_2\text{O}_3/\text{SiO}_2$ ratio of 0.4 were constructed by experiments. The examples of the phase diagrams and their applications are reviewed below.

3.1. $\text{CaO-MgO-Al}_2\text{O}_3\text{-SiO}_2$ System at Constant Al_2O_3 Content

446 compositions were studied by Osborn et al. [6] to construct pseudo-ternary sections CaO-MgO-SiO_2 with constant Al_2O_3 concentrations of 5 to 35% at 5% intervals. The conventional quenching experiments followed by the metallographic analysis were used in this study. Figure 3 shows the representation of the pseudo-ternary phase diagrams CaO-MgO-SiO_2 with constant Al_2O_3 concentrations of 10, 15 and 20%.

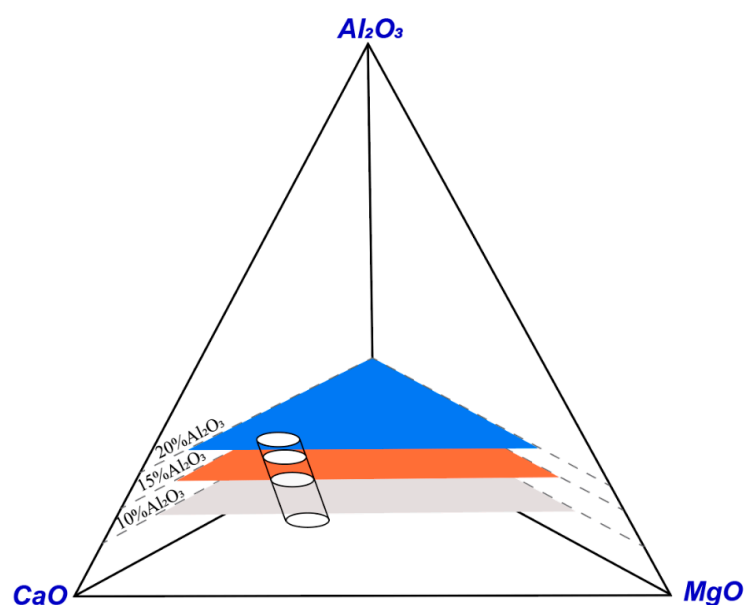


Figure 3. Representation of the pseudo-ternary phase diagrams CaO-MgO-SiO_2 with constant Al_2O_3 concentrations of 10, 15 and 20% [7].

Figures 4–6 show the experimentally determined pseudo-ternary phase diagrams CaO-MgO-SiO₂ at constant Al₂O₃ concentrations of 10, 15 and 20%, respectively. In these phase diagrams, the solid thick lines and thin lines represent the boundary lines and isotherms, respectively, determined by the experimental results. The dashed lines thick lines and thin lines represent the boundary lines and isotherms, respectively, by estimations. The primary phases identified in the composition range investigated include spinel (MgAl₂O₄), merwinite (Ca₃MgSi₂O₈), dicalcium silicate (Ca₂SiO₄), periclase (MgO), melilites (solid solutions of akermanite, Ca₂MgSi₂O₇, and gehlenite, Ca₂Al₂SiO₇), pseudo-wollastonite (CaSiO₃), anorthite (CaAl₂Si₂O₈), pyroxenes (predominantly solid solutions of clinoenstatite, MgSiO₃, and diopside, CaMgSi₂O₆), monticellite (CaMgSiO₄) and forsterite (Mg₂SiO₄). The Al₂O₃ in a BF slag is mainly from iron ores. A slag with 10% Al₂O₃ represents the use of high-quality iron ores which is rare at present. Then, 15% Al₂O₃ is an average for most of the current BF slag compositions. When low-quality and cheap iron ores are used, a BF slag containing 20% Al₂O₃ is generated. When Al₂O₃ in the slag is increased from 10 to 15%, the monticellite primary phase field is replaced by the spinel. Further, increase in Al₂O₃ to 20%, the size of the spinel primary phase field is expanded significantly. By considering liquidus temperature, desulphurization potential and viscosity, Osborn et al. proposed an “optimum” BF slag composition for each pseudo-ternary section. For example, at 10% Al₂O₃, the “optimum” slag contains 14% MgO, 44% CaO and 32% SiO₂. When the Al₂O₃ is increased to 20%, the “optimum” slag composition is changed to 11% MgO, 45% CaO and 24% SiO₂. However, these suggested “optimum” slag compositions were not used by the BF operators as they are too close to the MgO and Ca₂SiO₄ primary phase fields where the liquidus temperatures are very sensitive to the slag composition. A small increase in CaO or MgO concentration can increase the liquidus temperature significantly. Another issue is a higher slag rate for the “optimum” slag compositions because more CaO and MgO fluxes need to be added. In fact, each blast furnace has its own feed structure, hot metal quality requirement and operating parameters. The purpose of a phase diagram is to provide systematic information for all BF operators to select the composition suitable for their operations. It is not necessary for the researchers to recommend an “optimum” composition for BF slag.

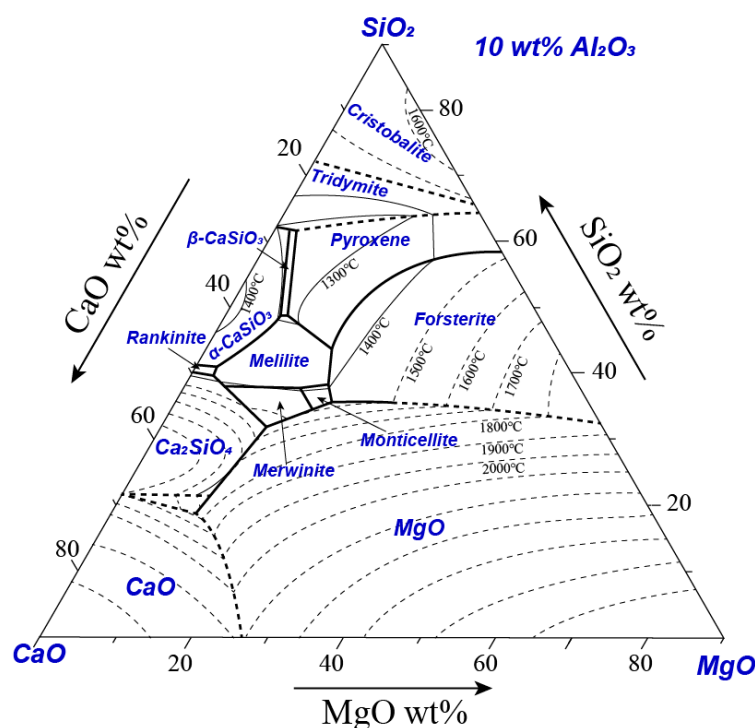


Figure 4. Pseudo-ternary phase diagram CaO-MgO-Al₂O₃-SiO₂ for the 10% Al₂O₃ plane [7].

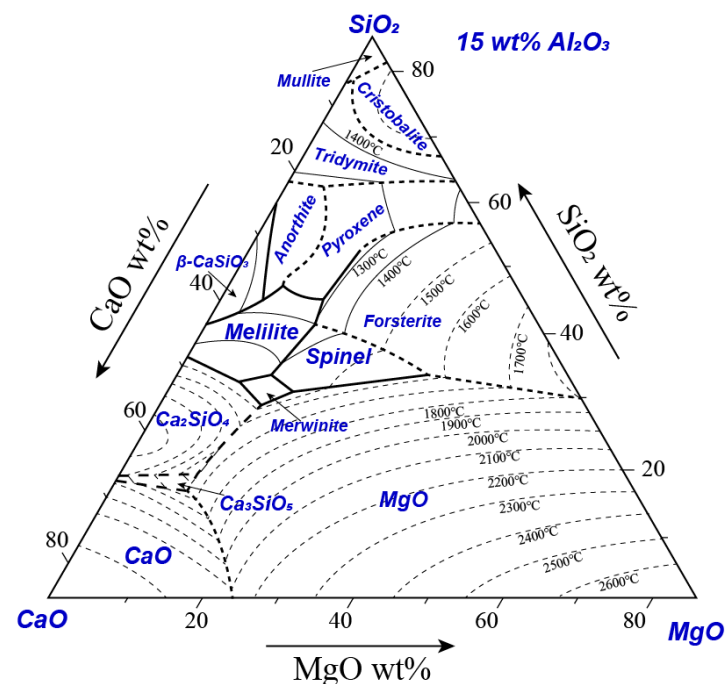


Figure 5. Pseudo-ternary phase diagram CaO-MgO-Al₂O₃-SiO₂ for the 15% Al₂O₃ plane [7].

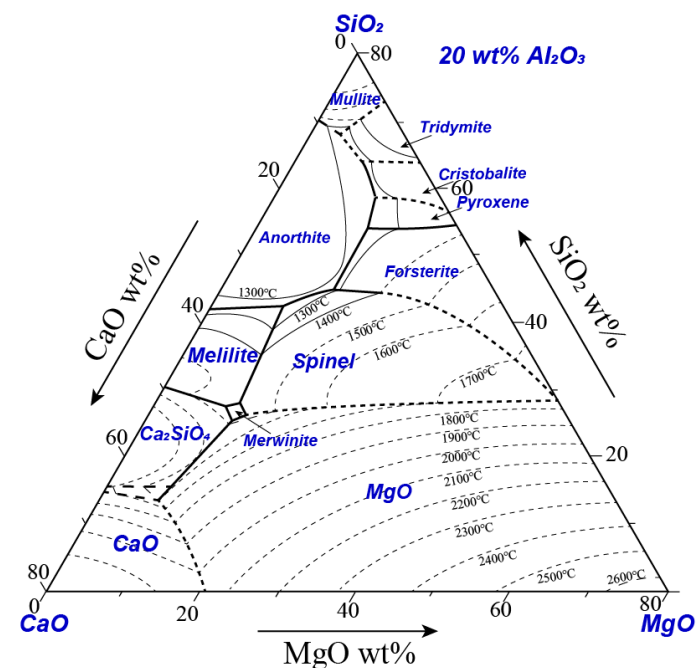


Figure 6. Pseudo-ternary phase diagram CaO-MgO-Al₂O₃-SiO₂ for the 20% Al₂O₃ plane [7].

3.2. CaO-MgO-Al₂O₃-SiO₂ System with Fixed MgO

To add knowledge to the phase equilibria of the system CaO-MgO-Al₂O₃-SiO₂ relevant to BF slags, Prince et al. [8] constructed a pseudo-ternary phase diagram CaO-MgO-Al₂O₃-SiO₂ at constant 10% MgO. He used conventional quenching and petrographic microscope technique to investigate the primary phase fields and liquidus temperatures as a function of composition. Figure 7 shows the pseudo-ternary phase diagram CaO-MgO-Al₂O₃-SiO₂ for the 10% MgO plane. It can be seen that the melilite primary phase field, which is usually the primary phase of a BF slag, is surrounded by the primary phase fields of spinel, merwinite, pseudo-wollastonite, diopside and anorthite. Unusual shapes of the isotherms in the melilite primary phase field indicate that the melilite solid solution is formed by two

endmembers: akermanite $\text{Ca}_2\text{MgSi}_2\text{O}_7$, and gehlenite $\text{Ca}_2\text{Al}_2\text{SiO}_7$. By using this diagram, at a constant MgO concentration in the slag, the effects of the CaO/SiO₂ ratio and Al₂O₃ on the liquidus temperature of the BF slag can be discussed by pseudo-binary phase diagrams from different directions.

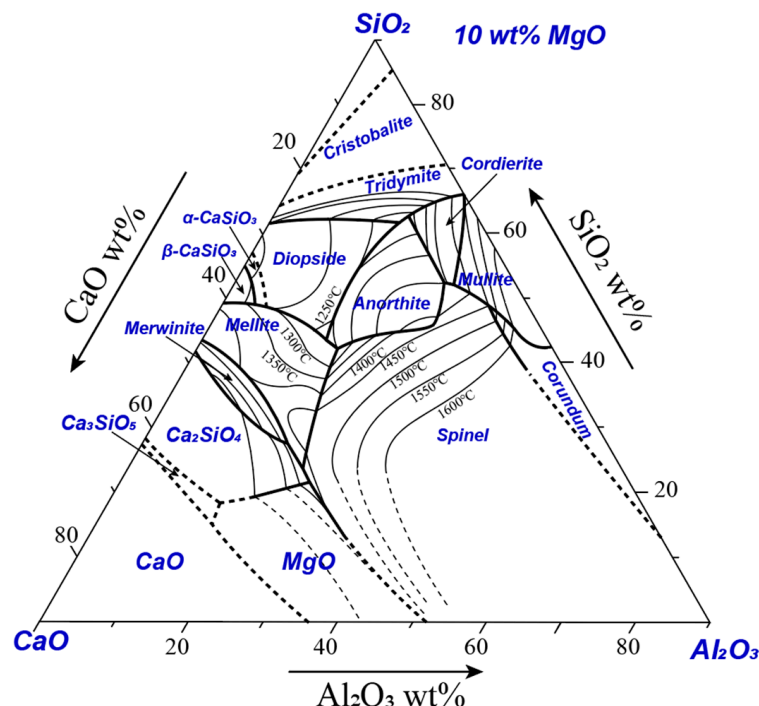


Figure 7. The 10% MgO plane of the system CaO-MgO-Al₂O₃-SiO₂ [8].

In a late study, Cavalier and Sandra-Deudon [10] reported three pseudo-ternary sections CaO-MgO-Al₂O₃-SiO₂ at constant 5, 10 and 15% MgO, respectively. They used a high-temperature microscopy technique to determine the liquidus temperature of a fused slag. The precipitation and growth of the primary and secondary phases can be observed directly by the hot-stage microscope. Their focus was to determine the phase boundaries and the isotherms were mainly estimated from the limited number of experiments. The high viscosity of the silicate slag could delay the precipitation of the solid phases and affect the accuracy of the results. The 10% MgO plane reported by Cavalier and Sandra-Deudon [10] is slightly below that reported by Prince [8]. For example, it can be seen from Figure 7 that the dicalcium silicate primary phase field joins with the melilite primary phase field. In the phase diagram reported by Cavalier and Sandra-Deudon [10], the dicalcium silicate primary phase field is separated from the melilite primary phase field by the merwinite primary phase field. The dicalcium silicate primary phase field in Figure 7 does not join with CaO primary phase field. However, in the phase diagram reported by Prince [8]. The dicalcium silicate primary phase field joins with CaO primary phase field at the low-Al₂O₃ area.

Gutt and Russell [11] reinvestigated the system CaO-MgO-Al₂O₃-SiO₂ at a constant 5% MgO using a hot-stage microscope technique. Figure 8 compares the results between Cavalier and Sandra-Deudon [10] and Gutt and Russell [11]. It can be seen that even though the same experimental technique was used, different primary phases and sizes of the primary phases were reported by the two groups. The C₆MA₄S phase reported by Gutt and Russell [11] is not present on the plane reported by Cavalier and Sandra-Deudon [10]. On the other hand, the merwinite primary phase field was not mentioned by Cavalier and Sandra-Deudon [10].

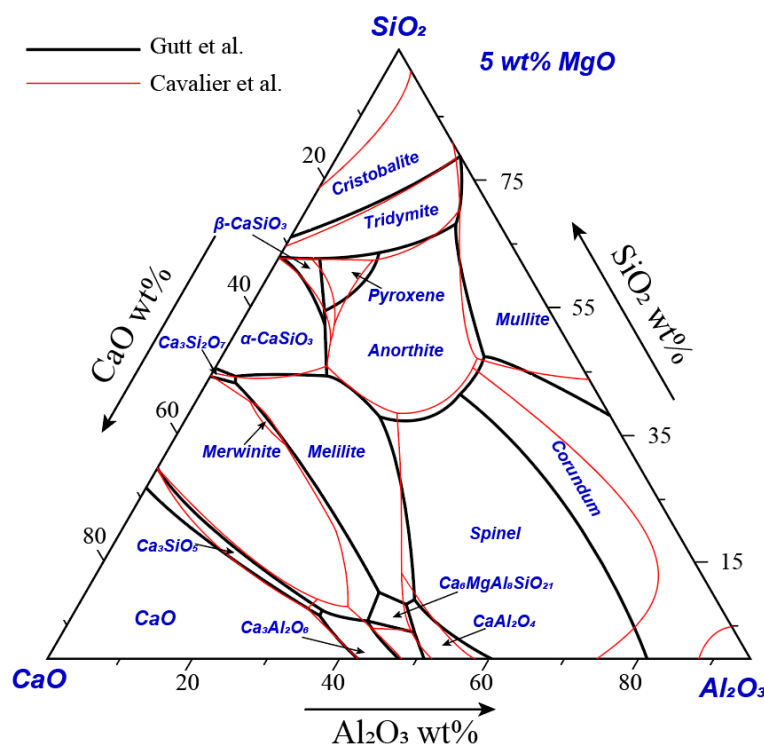


Figure 8. Comparison of the phase boundaries between Cavalier and Sandrea-Deudon [10] and Gutt and Russell [11].

3.3. $(\text{CaO} + \text{SiO}_2)\text{-Al}_2\text{O}_3\text{-MgO}$ System at Constant CaO/SiO_2

Binary basicity CaO/SiO_2 is a key parameter to determine the desulphurization capacity and viscosity of the BF slag, and the quality of hot metal. For a given BF, CaO/SiO_2 is usually kept constant to maintain a stable operation and hot metal quality. Following the requirements from BF operators, a series of pseudo-ternary phase diagrams $(\text{CaO} + \text{SiO}_2)\text{-Al}_2\text{O}_3\text{-MgO}$ at constant CaO/SiO_2 ratio were constructed by using the quenching-EPMA technique [13–16]. Figure 9 shows the representation of the pseudo-ternary phase diagrams $\text{CaO} + \text{SiO}_2\text{-Al}_2\text{O}_3\text{-MgO}$ at constant CaO/SiO_2 ratios. When CaO/SiO_2 ratio is fixed, $(\text{CaO}/\text{SiO}_2)$ can be taken as one of the end members in a pseudo-ternary phase diagram. Four pseudo-ternary sections with the CaO/SiO_2 ratios of 0.9, 1.1, 1.3 and 1.5 were constructed experimentally. The sections with the CaO/SiO_2 ratios 0.9–1.3 represent the composition range for the final BF slags and the section with the CaO/SiO_2 ratio of 1.5 represents the compositions of the bosh slag.

Figures 10–12 show three pseudo-ternary phase diagrams $(\text{CaO} + \text{SiO}_2)\text{-Al}_2\text{O}_3\text{-MgO}$ at constant CaO/SiO_2 ratios of 0.9, 1.1 and 1.3, respectively. It can be seen from Figure 10a that the melilite primary phase field in the new diagram shifted toward the low $\text{CaO} + \text{SiO}_2$ direction and the wollastonite primary phase field expands compared to the results from Slag Atlas [25]. It should be mentioned that the corundum primary phase field was revealed in the $\text{CaO-SiO}_2\text{-Al}_2\text{O}_3$ system which agrees with the present study, although the corundum primary phase field expands toward the high $\text{CaO} + \text{SiO}_2$ direction and the liquidus temperature from the previous study shows a large discrepancy with the current results. The liquidus temperatures obtained from Slag Atlas deviate largely from the present measurements in both ternary systems.

The calculated phase diagram by FactSage thermodynamic software is used to compare with the present results and is shown in Figure 10b. The comparisons of primary phase fields in Figure 9 show that FactSage reproduced the wollastonite, melilite, olivine, periclase, and spinel primary phase fields in the phase diagram, while the corundum primary phase field was not shown in the FactSage calculation. The area of the melilite primary phase field in the present study is narrowed by the expansion of wollastonite, olivine, and spinel

primary phase fields compared to the calculated diagram. Good agreements of isotherms were only found in the spinel primary field, while all the isotherms in periclase, olivine, melilite, and wollastonite changed significantly. The prediction also shows that the olivine primary phase field would become fully liquid at a temperature of 1400 °C; however, the present measurements identified a small area with a liquidus temperature higher than 1400 °C.

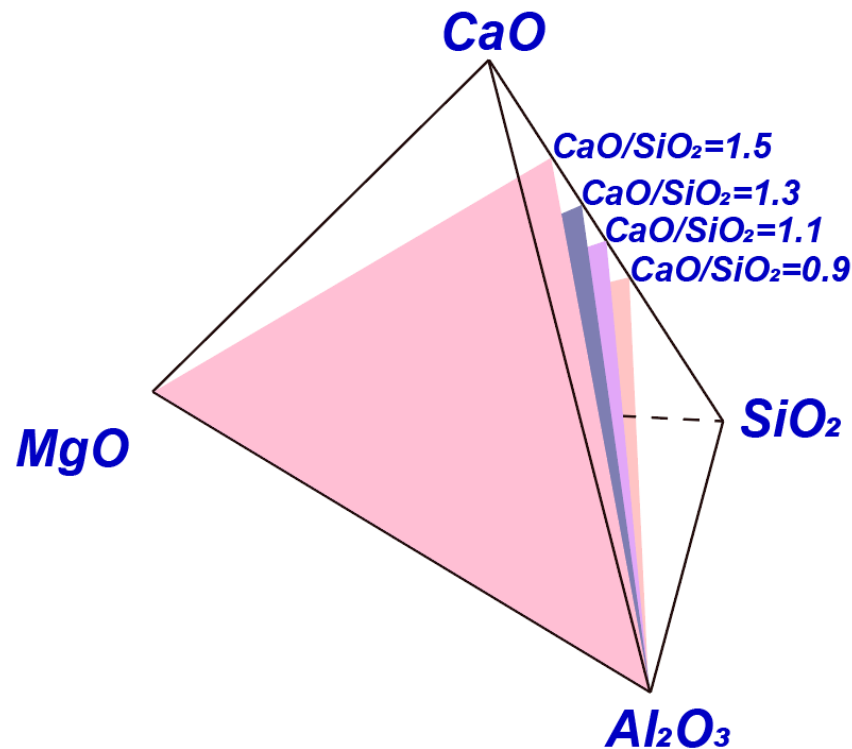


Figure 9. Representation of the pseudo-ternary phase diagrams (CaO + SiO₂)-Al₂O₃-MgO at constant CaO/SiO₂ ratios.

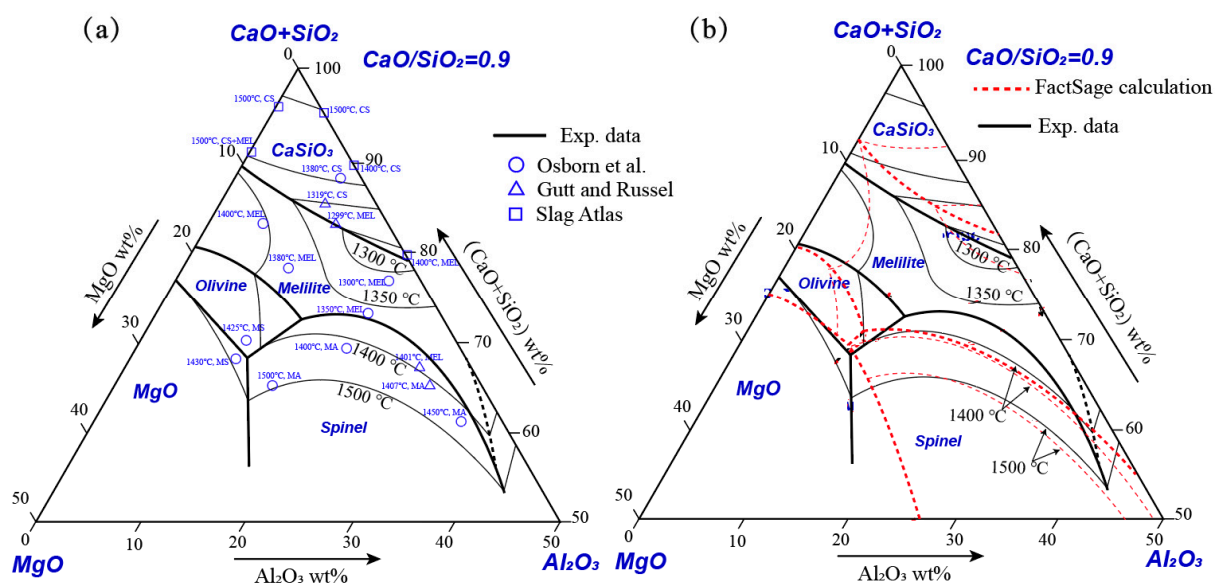


Figure 10. Experimentally determined pseudo-ternary phase diagram (CaO + SiO₂)-Al₂O₃-MgO at a constant CaO/SiO₂ ratio of 0.9 [13]. (a) Compare with the data reported by Osborn et al. [7], Gutt and Russel [11], and Slag Atlas [25], (b) compare with the FactSage prediction.

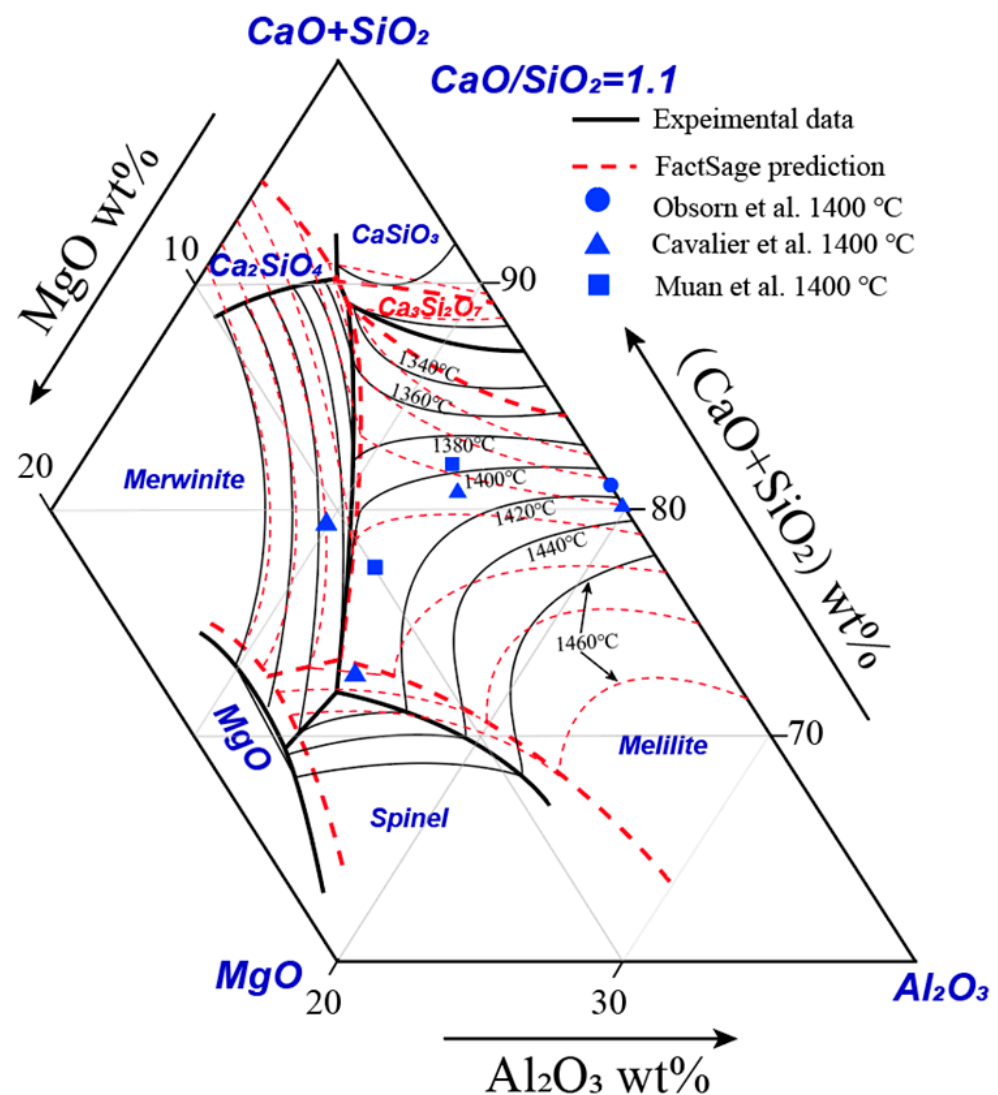


Figure 11. Experimentally determined pseudo-ternary phase diagram (CaO + SiO₂)-Al₂O₃-MgO at a constant CaO/SiO₂ ratio of 1.1 [14] compare with the data reported by Osborn et al. [7], Cavalier et al. [10], Muan et al. [24] and FactSage prediction.

It can be seen in Figure 11 that the experimental results have a good agreement with previous work reported by Osborn et al. [7], Cavalier and Sandra-Deudon [10] and Muan and Osborn [24] at 1400 °C. FactSage predictions show similar overall trends as the experimental results, but the locations of the isotherms can be found significantly different. The FactSage software used the published data to optimize the databases and the accuracy of FactSage calculations relies on the accuracy of the experimental data used. The deviation of FactSage can be attributed to the limitation of the previous research techniques so the accuracy of the data was not enough, in particular the solid solutions. Generally, the experimentally determined liquidus temperatures in the present study are approximately 20 °C higher than those FactSage predictions in the melilite primary phase field. In MgO and spinel primary phase fields, the experimentally determined liquidus temperatures in the present study are usually 20 °C lower than the predictions. In the merwinite primary phase field, the experimentally determined liquidus temperatures agree well with the prediction values. It is noted that there is a small Ca₃Si₂O₇ primary phase field according to the FactSage predictions. However, the Ca₃Si₂O₇ primary phase was not observed in the present study. Instead, the wollastonite (CaSiO₃) primary phase field is present in the

composition range. Additionally, the Ca_2SiO_4 primary phase was observed by the present experiments at the high $(\text{CaO} + \text{SiO}_2)$ corner, which is not shown by FactSage predictions.

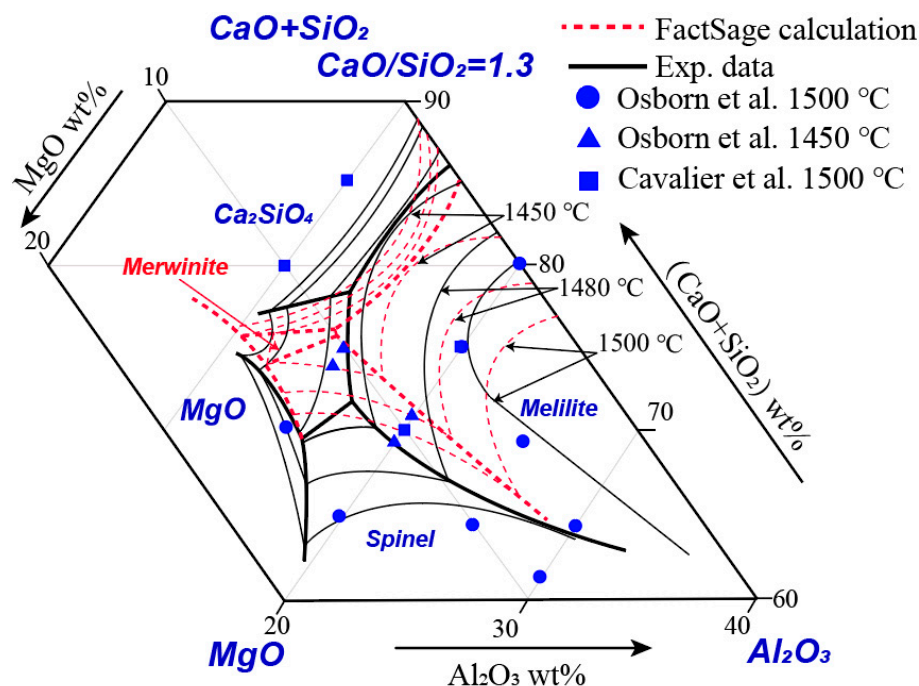


Figure 12. Experimentally determined pseudo-ternary phase diagram $(\text{CaO} + \text{SiO}_2)$ - Al_2O_3 - MgO at a constant CaO/SiO_2 ratio of 1.3 [15] compare with the data reported by Osborn et al. [7], Cavalier et al. [10] and FactSage prediction.

Figure 12 shows the experimentally determined pseudo-ternary phase diagram $(\text{CaO} + \text{SiO}_2)$ - Al_2O_3 - MgO at a constant CaO/SiO_2 ratio of 1.3 [15] compared with the data reported by Osborn et al. [7], Cavalier and Sandra-Deudon [10] and FactSage prediction. The experimental results show general agreement with previous works. The liquidus temperatures in the Ca_2SiO_4 primary phase field reported by Osborn et al. [7] are much higher than the present results. In addition, predictions of FactSage are also shown in the figure for comparison. FactSage predictions show similar trends as the experimental results, but the locations of the isotherms are significantly different. Experimentally determined liquidus temperatures in the spinel and Ca_2SiO_4 primary phase fields are approximately 50 °C lower than those predicted by FactSage. However, in the merwinite primary phase field, the experimentally determined liquidus temperatures are approximately 50 °C higher than the predictions. A significant difference is that the experimentally determined merwinite phase area is larger than the FactSage predictions. This significant difference may come from the lack of thermodynamics data in the merwinite primary phase field. In the melilite primary phase field, the experimentally determined liquidus temperatures are usually 20 °C different from predicted values.

3.4. CaO - MgO - Al_2O_3 - SiO_2 System at Constant $\text{Al}_2\text{O}_3/\text{SiO}_2$ or MgO/CaO

Al_2O_3 and SiO_2 in a BF slag come from raw materials that are usually fixed as the suppliers are relatively stable. The important variable parameter to adjust the slag properties is MgO/CaO which is added as flux. A pseudo-ternary phase diagram CaO - MgO - $(\text{Al}_2\text{O}_3 + \text{SiO}_2)$ at a constant $\text{Al}_2\text{O}_3/\text{SiO}_2$ ratio was reported by Liao et al. [22]. The quenching and EPMA technique was used to construct the pseudo-ternary plane as indicated in Figure 13. CaO , MgO and $(\text{Al}_2\text{O}_3 + \text{SiO}_2)$ are the end members of the plane. A constant $\text{Al}_2\text{O}_3/\text{SiO}_2$ ratio of 0.4 enables the $(\text{Al}_2\text{O}_3 + \text{SiO}_2)$ to be considered as one component.

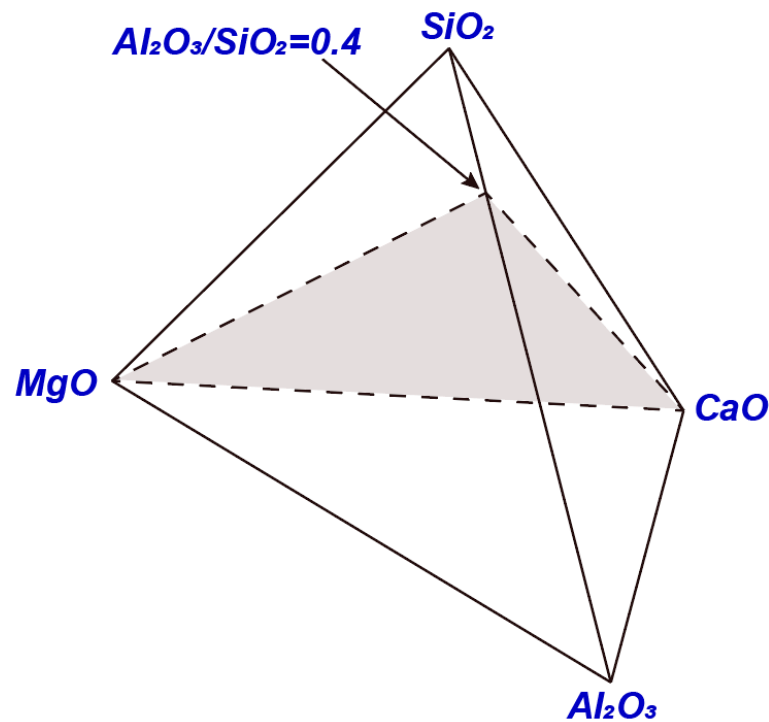


Figure 13. Representation of the pseudo-ternary phase diagram CaO-MgO-($\text{Al}_2\text{O}_3 + \text{SiO}_2$) at constant $\text{Al}_2\text{O}_3/\text{SiO}_2$ ratios [22].

The experimentally determined pseudo-ternary phase diagram is shown in Figure 14. A typical BF slag composition is also shown in the figure. It can be seen that this BF slag is in the melilite primary phase field with a liquidus temperature of approximately 1420 °C. A series of the pseudo-binary phase diagrams have been constructed from the pseudo-ternary to discuss the effects of MgO/CaO ratio and quaternary basicity $(\text{CaO} + \text{MgO})/(\text{Al}_2\text{O}_3 + \text{SiO}_2)$ on liquidus temperatures of the BF slags.

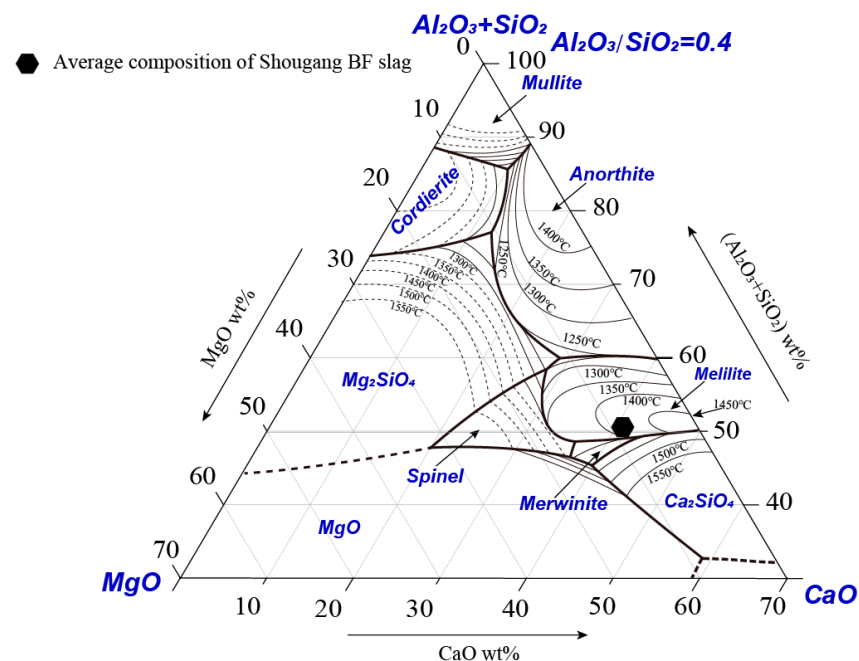


Figure 14. Experimentally determined pseudo-ternary phase diagram CaO-MgO-($\text{Al}_2\text{O}_3 + \text{SiO}_2$) at a constant $\text{Al}_2\text{O}_3/\text{SiO}_2$ ratio of 0.4 [22].

Figure 15 shows an example of the pseudo-binaries where the liquidus temperatures are presented as a function of the MgO/CaO ratio at constant ($\text{Al}_2\text{O}_3 + \text{SiO}_2$) of 50 and 55 wt%, respectively. FactSage predictions are also shown in the figure for comparison. The figure shows that melilite is the primary phase at a low MgO/CaO ratio and spinel is the primary phase at a high MgO/CaO ratio. The liquidus temperatures decrease in the melilite primary phase field and increase in the spinel primary phase field with increasing MgO/CaO ratio. The liquidus temperatures at high ($\text{Al}_2\text{O}_3 + \text{SiO}_2$) concentration (55 wt%) are always higher than those at low ($\text{Al}_2\text{O}_3 + \text{SiO}_2$) concentration (50 wt%). It is possible to decrease the liquidus temperature of the BF slag by increasing the MgO/CaO until it reaches the spinel primary phase field. The sizes of the melilite and spinel primary phase fields from the experimental results are much larger than those predicted by FactSage. In some areas, a 100 °C difference in the liquidus temperature is present between the experimental results and FactSage predictions.

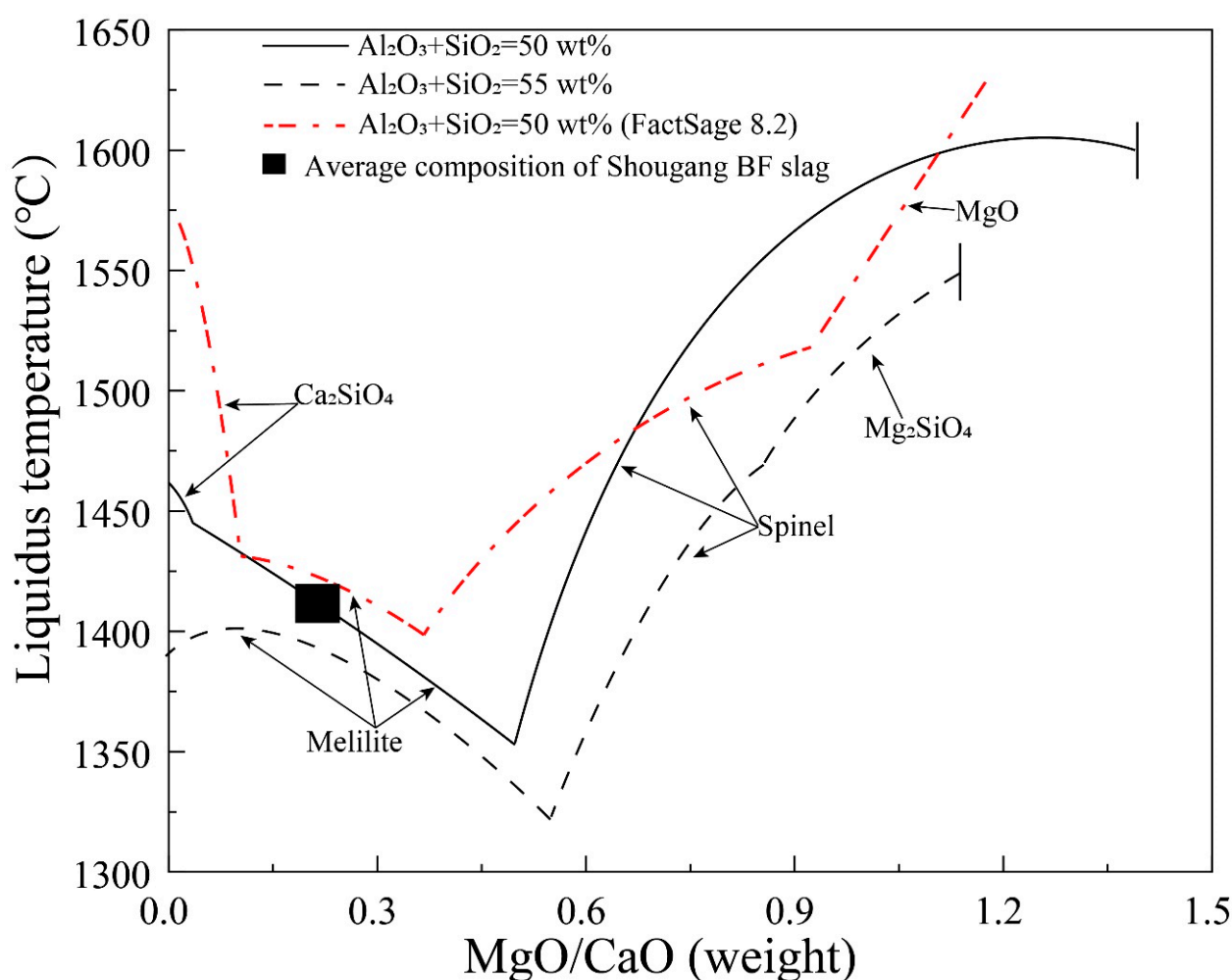


Figure 15. Liquidus temperature as a function of MgO/CaO in liquids at fixed ($\text{Al}_2\text{O}_3 + \text{SiO}_2$) of 50 and 55 wt% in the CaO-MgO-SiO₂-Al₂O₃ system with $\text{Al}_2\text{O}_3/\text{SiO}_2$ weight ratio of 0.4 [22].

The raw materials for a BF are not always fixed, in particular for the small BFs. It is important to understand the effect of variation in the raw materials on liquidus temperatures of the BF slags. Figure 16 indicates a pseudo-ternary phase diagram (CaO + MgO)-SiO₂-Al₂O₃ system at a constant MgO/CaO = 0.2. The end members are Al₂O₃, SiO₂ and (CaO + MgO) which enable the effect of raw material composition on liquidus temperatures of the BF slags to be discussed [23].

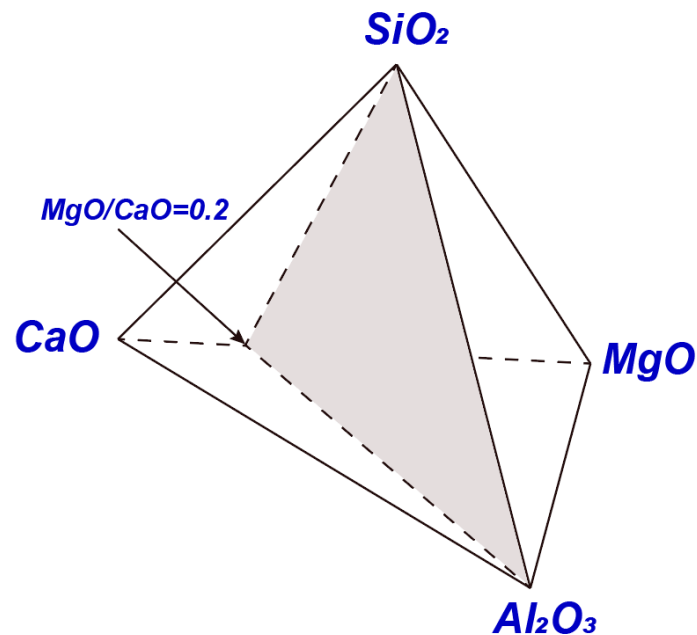


Figure 16. Representation of the pseudo-ternary phase diagrams (CaO + MgO)-Al₂O₃ + SiO₂ at a constant MgO/CaO ratio of 0.2 [23].

An experimentally determined pseudo-ternary phase diagram (CaO + MgO)-Al₂O₃-SiO₂ with a constant MgO/CaO ratio of 0.2 is shown in Figure 17. A typical BF slag composition and four special points are also shown in the figure. When the compositions of the iron ores and coke/coal vary, the Al₂O₃ and SiO₂ contents in the BF slag will change accordingly. Based on Figure 17, the effects of Al₂O₃ concentration, ternary and quaternary basicity and Al₂O₃/SiO₂ on the liquidus temperature of the BF slags were discussed from different directions.

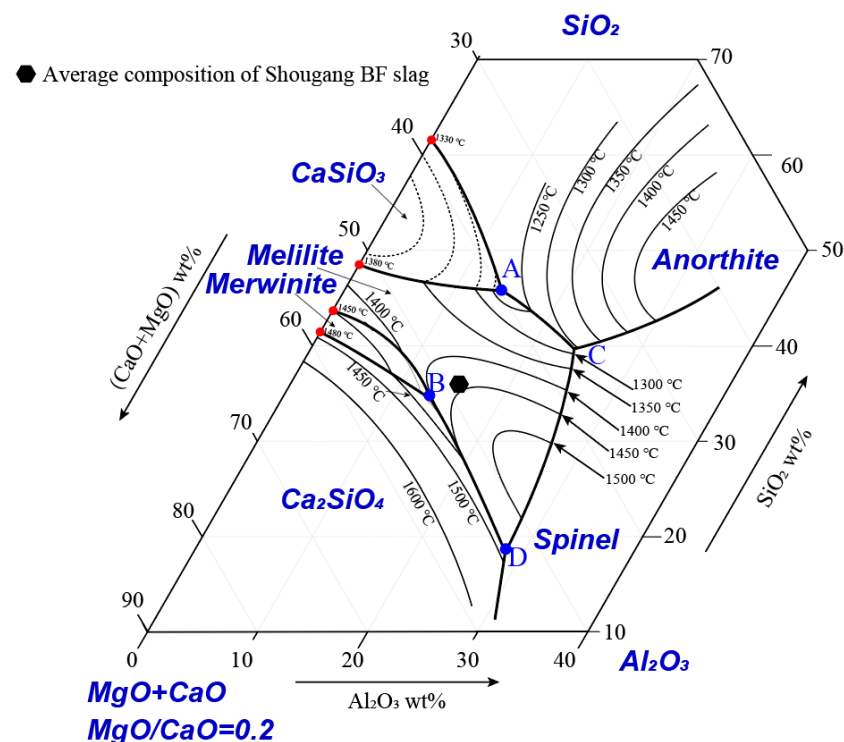


Figure 17. Experimentally determined pseudo-ternary phase diagram (CaO + MgO)-Al₂O₃-SiO₂ at a constant MgO/CaO ratio of 0.2 [23].

Figure 18 shows the liquidus temperatures of the BF slag as a function of $(\text{CaO} + \text{MgO})/\text{SiO}_2$ at content 10, 15 and 20 wt% Al_2O_3 . Melilite and Ca_2SiO_4 are the main primary phases present around the typical BF slag. When high-grade feeds are available, the Al_2O_3 content in the BF slag is low (10%), and the liquidus temperatures increase continuously with increasing $(\text{CaO} + \text{MgO})/\text{SiO}_2$ in all primary phase fields investigated. In the sections with 15 and 20% Al_2O_3 , the liquidus temperatures first increase and then decrease with increasing $(\text{CaO} + \text{MgO})/\text{SiO}_2$ in the anorthite and melilite primary phase fields. In the Ca_2SiO_4 primary phase field, the liquidus temperatures increase sharply with increasing $(\text{CaO} + \text{MgO})/\text{SiO}_2$. High basicity BF slag can decrease the sulphur content in the hot metal. However, the basicity is limited by the formation of the Ca_2SiO_4 phase where the liquidus temperatures are sensitive to the slag composition. At ternary basicity 1.32–1.40 which is the most common one in the current BF operation, the slag composition with 10% Al_2O_3 is close to the Ca_2SiO_4 primary phase field with the liquidus temperature below 1414 °C. At the same basicity, the BF slag has a liquidus temperature of 1427 and 1475 °C, respectively, corresponding to 15 and 20% Al_2O_3 . It can be seen from the figure that the ternary basicity can be further increased up to 1.6 at 15% Al_2O_3 with lower liquidus temperatures. When 20% Al_2O_3 is present in the slag, the ternary basicity can be further increased up to 1.8 without the formation of the Ca_2SiO_4 phase.

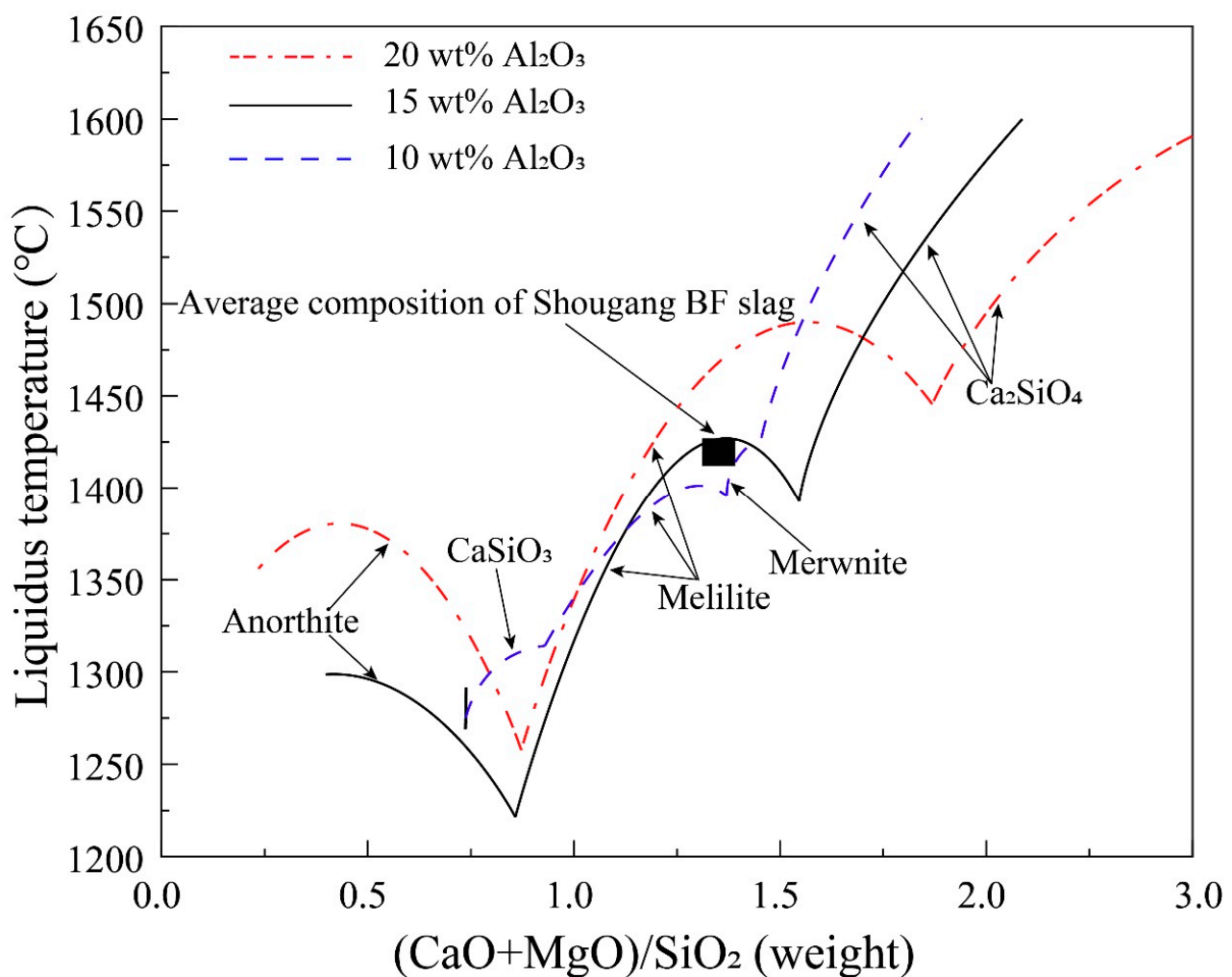


Figure 18. Liquidus temperature as a function of quaternary basicity at fixed MgO/CaO and $\text{Al}_2\text{O}_3/\text{SiO}_2$ ratios [23].

4. Comparison between Experimental Results and Thermodynamic Predictions

CALPHAD (CALculation of PHase Diagram) approach is the future to predict liquidus temperatures for metallurgical slags. FactSage is one of the most powerful thermodynamic packages for the BF slags. The accuracy of the thermodynamic predictions relies on the reliable experimental data used for the optimization of the database. Evaluation of the thermodynamic predictions by experimental data is of great significance for optimizing thermodynamic databases and avoiding misleading industrial practices. Figure 19 shows the liquidus temperatures of the BF slag as a function of Al_2O_3 concentration at constant ternary basicity of 1.2, 1.4 and 1.6. FactSage predicted liquidus temperatures at a ternary basicity of 1.4 are also shown in the figure for comparison. Melilite, merwinite and dicalcium silicate are the primary phases in the composition range investigated. An optimum Al_2O_3 concentration exists for constant ternary basicity. The lowest liquidus temperatures of 1360, 1380 and 1398 °C can be obtained at 8, 11.5 and 14.4% Al_2O_3 , respectively, for the ternary basicity of 1.2, 1.4 and 1.6. The predicted section of $(\text{MgO} + \text{CaO})/\text{SiO}_2 = 1.4$ by FactSage 8.2 is significantly different from the experimental results at the low Al_2O_3 area. Dicalcium silicate is predicted to be the primary phase at low Al_2O_3 concentrations. However, merwinite was reported to be the primary phase in the same composition range by experiments [23]. The liquidus temperatures predicted by FactSage are up to 120 °C higher than that of experimental results. The difference between the predictions and experimental data indicates that the current thermodynamic databases need to be further optimised. The possible reasons causing the inaccurate predictions were discussed by Liao et al. [23].

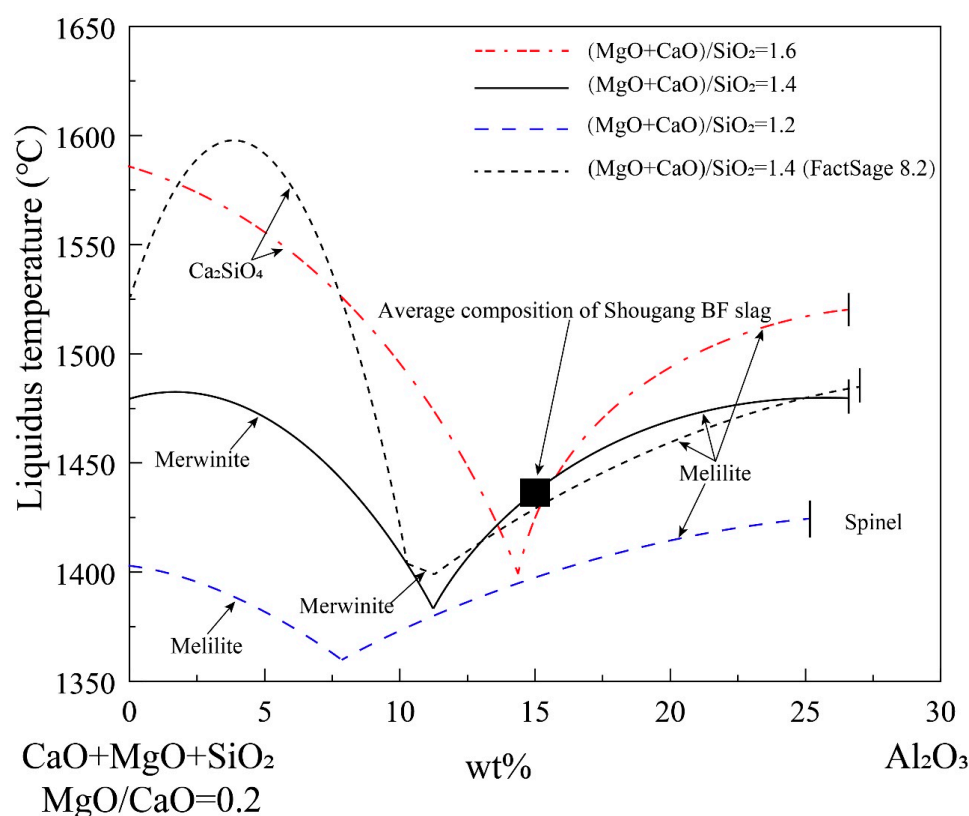


Figure 19. Liquidus temperature as a function of Al_2O_3 concentration at fixed ternary basicity $(\text{MgO} + \text{CaO})/\text{SiO}_2 = 1.2, 1.4$ and 1.6 [23].

The compositions of the BF slag are usually located in the melilite primary phase field. Melilite is the solid solution between akermanite ($2\text{CaO} \cdot \text{MgO} \cdot 2\text{SiO}_2$) and gehlenite ($2\text{CaO} \cdot \text{Al}_2\text{O}_3 \cdot \text{SiO}_2$). It can be seen from Figure 20 that the mol% of gehlenite ($2\text{CaO} \cdot \text{Al}_2\text{O}_3 \cdot \text{SiO}_2$) in predicted melilite is different from that in the experimentally measured melilite. It

seems that the predicted mol fractions of gehlenite in melilite have the same trend as the experimental data. However, a maximum difference of 23.4 mol% is observed between the predictions and experimental results. Unfortunately, there is no clear correlation between the difference of the gehlenite in melilite and the difference in the liquidus temperature.

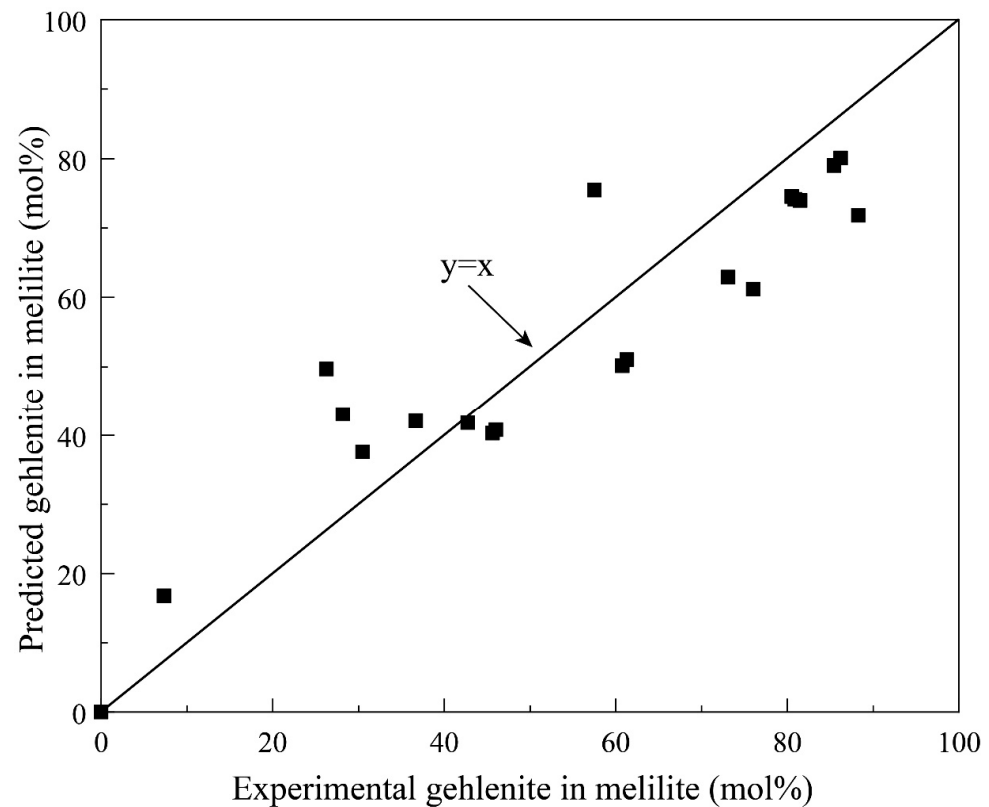


Figure 20. Comparison of the melilite composition between experimental data and FactSage predictions [23].

5. Conclusions

Research techniques and results of the phase equilibria for blast furnace ironmaking slags have been critically reviewed and summarised. Improved research techniques can produce complex phase diagrams more efficiently and accurately. The accurate solid solution measurements enabled the thermodynamic databases to be developed and optimised. Reduced quality of the raw materials and increased blast furnace technologies require more detailed phase diagrams to support the accurate control of the operations. Experimentally determined pseudo-ternary and pseudo-binary phase diagrams in the system $\text{CaO-MgO-Al}_2\text{O}_3\text{-SiO}_2$ have provided useful information to support industrial operations. With the development of ironmaking technologies and variations of the feed structures, more phase diagrams in different presentations could be required. More and more accurate experimental data will also support the thermodynamic databases to be optimised to a high level.

Author Contributions: Methodology, B.Z.; Validation, B.Z.; Formal analysis, J.L.; Resources, G.Q.; Data curation, J.L.; Writing—original draft, J.L. and G.Q.; Writing—review and editing, B.Z.; Supervision, B.Z.; Project administration, B.Z. All authors have read and agreed to the published version of the manuscript.

Funding: This research received no external funding.

Data Availability Statement: Not applicable.

Acknowledgments: The authors would like to acknowledge Shougang Research Institute of Technology for providing financial support.

Conflicts of Interest: The authors declare no conflict of interest.

References

- Wang, Y.; Zuo, H.; Zhao, J. Recent progress and development of ironmaking in China as of 2019: An overview. *Ironmak. Steelmak.* **2020**, *47*, 640–649. [\[CrossRef\]](#)
- Geerdes, M.; Chaigneau, R.; Lingardi, O. *Modern Blast Furnace Ironmaking: An Introduction, Chapter XI- Operation Challenges*, 4th ed.; IOS Press: Amsterdam, The Netherlands, 2020.
- Zhang, X.; Jiao, K.; Zhang, J.; Guo, Z. A review on low carbon emissions projects of steel industry in the world. *J. Clean. Prod.* **2021**, *306*, 127259. [\[CrossRef\]](#)
- Mousa, E. Modern blast furnace ironmaking technology: Potentials to meet the demand of high hot metal production and lower energy consumption. *Metall. Mater. Eng.* **2019**, *25*, 69–104. [\[CrossRef\]](#) [\[PubMed\]](#)
- Osborn, E.F.; Schairer, J.F. The ternary system pseudo wollastonite-akermanite-gehlenite. *Am. J. Sci.* **1941**, *239*, 715–763. [\[CrossRef\]](#)
- Prince, A. Phase equilibrium relationships in a portion of the system $\text{MgO-Al}_2\text{O}_3\text{-2CaO-SiO}_2$. *J. Am. Ceram. Soc.* **1951**, *34*, 44–51. [\[CrossRef\]](#)
- Osborn, E.F.; DeVries, R.C.; Gee, K.H.; Kraner, H.M. Optimum composition of blast furnace slag as deduced for the quaternary system $\text{CaO-MgO-Al}_2\text{O}_3\text{-SiO}_2$. *Trans. AIME* **1954**, *6*, 33–45. [\[CrossRef\]](#)
- Prince, A. Liquidus relationships on 10% MgO plane of the system lime-magnesia-alumina-silica. *J. Am. Ceram. Soc.* **1954**, *37*, 402–408. [\[CrossRef\]](#)
- DeVries, R.C.; Osborn, E.F. Phase equilibria in High-alumina part of the system $\text{CaO-MgO-Al}_2\text{O}_3\text{-SiO}_2$. *J. Am. Ceram. Soc.* **1957**, *40*, 6–15. [\[CrossRef\]](#)
- Cavalier, G.; Sandrea-Deudon, M. Quaternary slags $\text{CaO-MgO-Al}_2\text{O}_3\text{-SiO}_2$: Liquidus surfaces and crystallization paths for constant magnesia concentrations. *Rev. Metall.* **1960**, *5*, 1143–1157. [\[CrossRef\]](#)
- Gutt, W.; Russel, A.D. Studies of the system $\text{CaO-SiO}_2\text{-Al}_2\text{O}_3\text{-MgO}$ in relation to the stability of blast furnace slag. *J. Mater. Sci.* **1977**, *12*, 1869–1878. [\[CrossRef\]](#)
- Dahl, F.; Brandberg, J.; Du, S. Characterization of melting of some slags in the $\text{Al}_2\text{O}_3\text{-CaO-MgO-SiO}_2$ quaternary system. *ISIJ Int.* **2006**, *46*, 614–616. [\[CrossRef\]](#)
- Wang, D.; Chen, M.; Jiang, Y.; Wang, S.; Zhao, Z.; Evans, T.; Zhao, B. Phase equilibria studies in the $\text{CaO-SiO}_2\text{-Al}_2\text{O}_3\text{-MgO}$ system with CaO/SiO_2 ratio of 0.9. *J. Am. Ceram. Soc.* **2020**, *103*, 7299–7309. [\[CrossRef\]](#)
- Ma, X.; Zhang, D.; Zhao, Z.; Evans, T.; Zhao, B. Phase equilibria studies in the $\text{CaO-SiO}_2\text{-Al}_2\text{O}_3\text{-MgO}$ system with CaO/SiO_2 ratio of 1.10. *ISIJ Int.* **2016**, *56*, 513–519. [\[CrossRef\]](#)
- Ma, X.; Wang, G.; Wu, S.; Zhu, J.; Zhao, B. Phase equilibria in the $\text{CaO-SiO}_2\text{-Al}_2\text{O}_3\text{-MgO}$ System with CaO/SiO_2 ratio of 1.3 relevant to iron blast furnace slags. *ISIJ Int.* **2015**, *55*, 2310–2317. [\[CrossRef\]](#)
- Kou, M.; Wu, S.; Ma, X.; Wang, L.; Chen, M.; Cai, Q.; Zhao, B. Phase equilibrium studies of $\text{CaO-SiO}_2\text{-Al}_2\text{O}_3\text{-MgO}$ system with binary basicity of 1.5 related to blast furnace slag. *Metall. Mater. Trans. B* **2016**, *47*, 1093–1102. [\[CrossRef\]](#)
- Gran, J.; Wang, Y.; Du, S. Experimental determination of the liquidus in the high basicity region in the Al_2O_3 (30 mass%)- CaO-MgO-SiO_2 system. *Calphad* **2011**, *35*, 249–254. [\[CrossRef\]](#)
- Gran, J.; Yan, B.; Du, S. Experimental determination of the liquidus in the high-basicity region in the Al_2O_3 (25 mass pct)- CaO-MgO-SiO_2 and Al_2O_3 (35 mass pct)- CaO-MgO-SiO_2 systems. *Metall. Mater. Trans. B* **2011**, *42*, 1008–1016. [\[CrossRef\]](#)
- Lyu, S.; Ma, X.; Chen, M.; Huang, Z.; Wang, G. Application of phase equilibrium studies of $\text{CaO-SiO}_2\text{-Al}_2\text{O}_3\text{-MgO}$ system for oxide inclusions in Si-deoxidized steels. *Calphad* **2020**, *68*, 101721. [\[CrossRef\]](#)
- Lyu, S.; Ma, X.; Huang, Z.; Yao, Z.; Lee, H.; Jiang, Z.; Wang, G.; Zou, J.; Zhao, B. Inclusion characterization and formation mechanisms in spring steel deoxidized by silicon. *Metall. Mater. Trans. B* **2019**, *5*, 732–747. [\[CrossRef\]](#)
- Yao, Z.; Ma, X.; Lyu, S. Phase equilibria of the $\text{Al}_2\text{O}_3\text{-CaO-SiO}_2\text{-(0%, 5%, 10%)} \text{MgO}$ slag system for non-metallic inclusions control. *Calphad* **2021**, *72*, 102227. [\[CrossRef\]](#)
- Liao, J.; Qing, G.; Zhao, B. Phase equilibria studies in the $\text{CaO-MgO-Al}_2\text{O}_3\text{-SiO}_2$ system with $\text{Al}_2\text{O}_3/\text{SiO}_2$ weight ratio of 0.4. *Metals* **2023**, *13*, 224. [\[CrossRef\]](#)
- Liao, J.; Qing, G.; Zhao, B. Phase equilibrium studies in the $\text{CaO-SiO}_2\text{-Al}_2\text{O}_3\text{-MgO}$ system with MgO/CaO ratio of 0.2. *Metall. Mater. Trans. B* **2023**, *54*, 793–806.
- Muan, A.; Osborn, E.F. *Phase Equilibria Among Oxides in Steelmaking*; Addison-Wesley Publishing Company: Boston, MA, USA, 1965; pp. 148–157.
- Verein Deutscher Eisenhüttenleute: Slag Atlas*; Verlag Stahleisen GmbH: Düsseldorf, Germany, 1995; Volume 156.
- Bale, C.W.; Bélisle, E.; Chartrand, P.; Decterov, S.; Eriksson, G.; Gheribi, A.; Hack, K.; Jung, I.H.; Kang, Y.B.; Melançon, J.; et al. Reprint of: FactSage thermochemical software and databases, 2010–2016. *Calphad* **2016**, *55*, 1–19. [\[CrossRef\]](#)
- Davies, R.; Dinsdale, A.; Gisby, J.; Robinson, J.; Martin, S. MTDATA-thermodynamic and phase equilibrium software from the national physical laboratory. *Calphad* **2002**, *26*, 229–271. [\[CrossRef\]](#)
- Andersson, J.; Helander, T.; Höglund, L.; Shi, P.; Sundman, B. Thermo-Calc & DICTRA, computational tools for materials science. *Calphad* **2002**, *26*, 273–312.
- Jak, E.; Hayes, P.; Lee, H. Improved methodologies for the determination of high temperature phase equilibria. *Met. Mater.* **1995**, *1*, 1–8. [\[CrossRef\]](#)
- Bowen, N.L.; Schairer, J.F.; Posnjak, E.B. The System $\text{Ca}_2\text{SiO}_4\text{-Fe}_2\text{SiO}_4$. *Am. J. Sci.* **1933**, *25*, 273–297. [\[CrossRef\]](#)

31. Bowen, S. The system FeO-SiO₂. *Am. J. Sci.* **1932**, *24*, 177–213. [[CrossRef](#)]
32. Jung, I.V.; Ende, M. Computational thermodynamic calculations: FactSage from CALPHAD thermodynamic database to virtual process simulation. *Metall. Mater. Trans. B* **2020**, *51*, 1851–1874. [[CrossRef](#)]
33. Centre for Research in Computational Thermochemistry. FactSage 8.2 News. 2022. Available online: https://www.factsage.com/FS82_news.HTM (accessed on 5 December 2022).

Disclaimer/Publisher's Note: The statements, opinions and data contained in all publications are solely those of the individual author(s) and contributor(s) and not of MDPI and/or the editor(s). MDPI and/or the editor(s) disclaim responsibility for any injury to people or property resulting from any ideas, methods, instructions or products referred to in the content.